Magnetic Resonance in Medicine 51:863–868 (2004)

Improved Combination of Spiral-In/Out Images for BOLD fMRI

Gary H. Glover* and Moriah E. Thomason

Acquisitions with the spiral-in/out technique result in two separate image timeseries obtained during the spiral-in and spiral-out trajectory. In uniform brain regions the two components have comparable signal and BOLD contrast and can be averaged, but in regions compromised by susceptibility effects where both signal and noise can differ in the two images other combination methods may be more effective. Here, several weighting schemes are compared for signal and activation contrast recovery in whole brain and prefrontal cortex using verbal working memory (seven subjects) and breathholding tasks (six subjects) scanned at 3 T. It was found that a statistically weighted combination based on activation maps derived separately from the spiral-in and spiral-out images provides activation volumes with increases of 33–59% over second-choice signal-weighted combination and 100–200% increases over spiral-out acquisition alone, and that simple averaging is inferior to signal-weighted combination. Magn Reson Med 51: 863–868, 2004. © 2004 Wiley-Liss, Inc.

Key words: functional MRI; spiral in/out acquisitions; fMRI combination methods

The spiral-in/out acquisition has been proposed to reduce the effect of macroscopic susceptibility-induced field gradients (SFGs) generated near air–tissue interfaces such as orbital frontal, medial temporal, and lateral parietal regions and to increase both signal-to-noise ratio (SNR) and BOLD contrast-to-noise ratio (CNR) in fMRI (1). In this technique, spiral-in and spiral-out timeseries are separately generated from each acquisition and combined in postprocessing. It was shown previously that the spiral-in images have increased signal relative to the spiral-out images in regions compromised by SFGs, and when combined with the spiral-out images can result in improved overall SNR and BOLD contrast (1,2). Previously, it was suggested that weighting of the two image series based on the signal in each voxel improved the resulting combination over simple averaging, but no comparison was performed and no other combination methods were explored.

Subsequently, we observed that not only can the signal intensities be different in the two images, but the timeseries variance as well, with the noise sometimes higher in the spiral-out image series even though the signal is lower than in the spiral-in image series, and vice versa. Thus, it was hypothesized that combinations of the spiral-in and spiral-out images could be further optimized if both signal and noise were considered in developing the weights used in the combination.

In this study we examined spiral-in/out combination methods using weighting functions for the spiral-in and spiral-out components based on simple averaging, signal amplitude, SNR, and BOLD CNR. Activation volumes obtained with these newer methods were compared to results from the signal-weighted combination used previously.

THEORY

Let $y_1(t)$ and $y_2(t)$ be the voxelwise timeseries signal intensities for spiral-in and spiral-out, respectively, and σ_1 and σ_2, the corresponding noise fluctuations. Because the origin of *k*-space is common for the two image timeseries the signal and noise are not fully independent, and in general there is a non-null component of covariance σ_{12} in the noise of each image. Such covariance can be expected when there is signal fluctuation due to physiological processes that have correlation times longer than the readouts, particularly at higher field (3,4) or with system instabilities. However, it has been shown that in uniform brain regions the SNR of averages of the two images at 3 T is ~1.3 times that of either the spiral-in or spiral-out image (1), which means that the covariance component is small ($\sqrt{2}$ would be expected for uncorrelated noise). With this motivation, we make the simplifying step of ignoring covariance, thereby assuming that the noise is fully uncorrelated.

An additional consideration when computing the timeseries noise is that activated voxels will have a variance component from the BOLD contrast itself. This component is assumed to be removed in σ_i, below.

Then, the combined signal y and noise σ is:

$$y = w_1 y_1 + w_2 y_2, \qquad [1]$$

$$\sigma^2 = w_1^2 \sigma_1^2 + w_2^2 \sigma_2^2, \qquad [2]$$

where w_i are combination weights that are constant in time, and $w_1 + w_2 = 1$.

Now we examine different weighting functions, defined independently for each voxel.

Simple Averaging ("Ave")

For simple averaging, $w_1 = w_2 = 0.5$. In this case, weighting of components in the combined image does not respect differences in signal intensities or noise between the two components. For voxels in which signal is lost in the spiral-out image but not for the spiral-in image, this com-

Department of Radiology and Neurosciences Program, Center for Advanced MR Technology at Stanford, Stanford University, Stanford, California.

Grant sponsor: NIH; Grant numbers: RR 09784; MH 63576; Grant sponsors: Lucas Foundation, GE Medical Systems.

*Correspondence to: Gary H. Glover, Ph.D., Stanford University School of Medicine, Lucas MR Center, 1201 Welch Road, Stanford, CA 94305-5488. E-mail: gglover@stanford.edu.

Received 17 July 2003; revised 14 November 2003; accepted 14 November 2003.

DOI 10.1002/mrm.20016

Published online in Wiley InterScience (www.interscience.wiley.com).

bination may not be ideal because in that case only noise is added by the spiral-out image.

Signal-Weighted Combination ("S-wt")

In signal-weighted combination, the relative contributions of spiral-in and spiral-out in each voxel are determined by the average signal intensity across time. Weights are linearly proportional to the timeseries mean signal in each image, and are given by:

$$w_1 = \bar{y}_1/(\bar{y}_1 + \bar{y}_2), \qquad [3]$$

where the overbars denote timeseries averages of the signals.

SNR-Weighted Combination ("SNR-wt")

For SNR-weighted combination, the relative contributions of spiral-in and spiral-out are found by maximizing the SNR of the combined timeseries, i.e., the average signal divided by the standard deviation across time. From Eqs. [1,2], the SNR is given by:

$$SNR \equiv \bar{y}/\sigma = \frac{w_1(\bar{y}_1 - \bar{y}_2) + \bar{y}_2}{[w_1^2\sigma_1^2 + (1 - w_1)^2\sigma_2^2]^{1/2}}. \qquad [4]$$

The weights that maximize SNR are given by setting $\partial(SNR)/\partial w_1 = 0$. One finds:

$$w_1 = \bar{y}_1\sigma_2^2/(\bar{y}_1\sigma_2^2 + \bar{y}_2\sigma_1^2). \qquad [5]$$

Note that if the timeseries noise is the same in the two images ($\sigma_1 = \sigma_2$), the weights are equivalent to S-wt, Eq. [3].

CNR-Weighted Combination ("CNR-wt")

In CNR-weighted combination, activation maps obtained separately from the spiral-in and spiral-out timeseries are used as the control input to the linear combination. In this work, activation maps are computed by cross correlation of each timeseries with a covariate *c(t)* generated by convolving the experimental task design timeseries with a suitable hemodynamic response function (HRF), and thus are proportional to the correlation coefficients r_I, given by:

$$r_i = \langle y_i \cdot c\rangle/(\sigma_i\sigma_c), \qquad [6]$$

where $\langle\ \rangle$ denotes the covariance operator and σ_c is the standard deviation of *c*. Then the activation map (cross-correlation coefficient *r*) of the combined timeseries is given by:

$$r = \langle y \cdot c\rangle/(\sigma\sigma_c). \qquad [7]$$

Substituting Eqs. [1] and [2] into Eq. [7], one has:

$$r = \frac{w_1(\sigma_1 r_1 - \sigma_2 r_2) + \sigma_2 r_2}{[w_1^2\sigma_1^2 + (1 - w_1)^2\sigma_2^2]^{1/2}}. \qquad [8]$$

The weights that maximize r are given by setting $\partial r/\partial w_1 = 0$. Then for BOLD CNR-wt:

$$w_1 = \sigma_1\sigma_2^2 r_1/(\sigma_1\sigma_2^2 r_1 + \sigma_2\sigma_1^2 r_2). \qquad [9]$$

Again, if the noise is the same in each timeseries, w_1 reduces to the simple linear combination of r_1 and r_2.

EXPERIMENTAL METHODS

Experiments were performed using spiral-in/out acquisitions during cognitive processing and, separately, during hypoxia induced by breathholding. The first task was chosen to enable comparisons in specific frontal regions where SFGs cause signal loss, while the second produced global BOLD responses that included the regions activated by the first task as well as most other gray matter voxels. The latter task thus served as a control because a robust gray matter BOLD response is achieved without depending on cognitive processing. Spiral-in/out activation maps were generated using the various combination methods for the two tasks and comparisons of activation volumes obtained for each of these methods were performed against the previously used signal-weighted method.

Acquisitions

Tasks

Seven subjects (age 19–42 years, mean 28.5 ± 8.8 years; five males, two females) performed a verbal working memory (VWM) task known to activate left prefrontal cortex (LPFC) (2). All subjects were right-handed, native English speakers who provided informed consent in accordance with a protocol approved by the Stanford Institutional Review Board. Following presentation of a fixation cross, subjects viewed a target set of five letters, and after WM delay viewed a sixth, probe letter. Eight experimental and eight control blocks each contained four 6-sec trials for a scan total of 192 volumes.

The second subject group (age 11.5–24.2 years, mean 16.1 ± 6.1 years; four males, two females, right-handed) were scanned during hypoxic challenge. Hypoxia was induced by alternating blocks of breathholding (BH) and self-paced breathing (5,6). During the 18-sec experimental condition, subjects held their breath after inspiration while viewing a circle that diminished in size until the block was concluded. The subjects breathed normally during the 18-sec control block. Seven experimental and seven control blocks were acquired for a total of 168 volumes.

MRI Acquisitions

All imaging data were acquired with a 3 T scanner (GE Signa, Milwaukee, WI; rev VH3.8) with either the manufacturer's quadrature birdcage head coil and foam padding (VWM task) or a smaller quadrature birdcage head coil with a bite bar (BH task). T_2-weighted FSE scans were obtained for anatomic reference (TR/TE/ETL = 4000ms/68ms/12, 5-mm interleaved contiguous slices, FOV = 24 cm, 192 × 256 matrix).

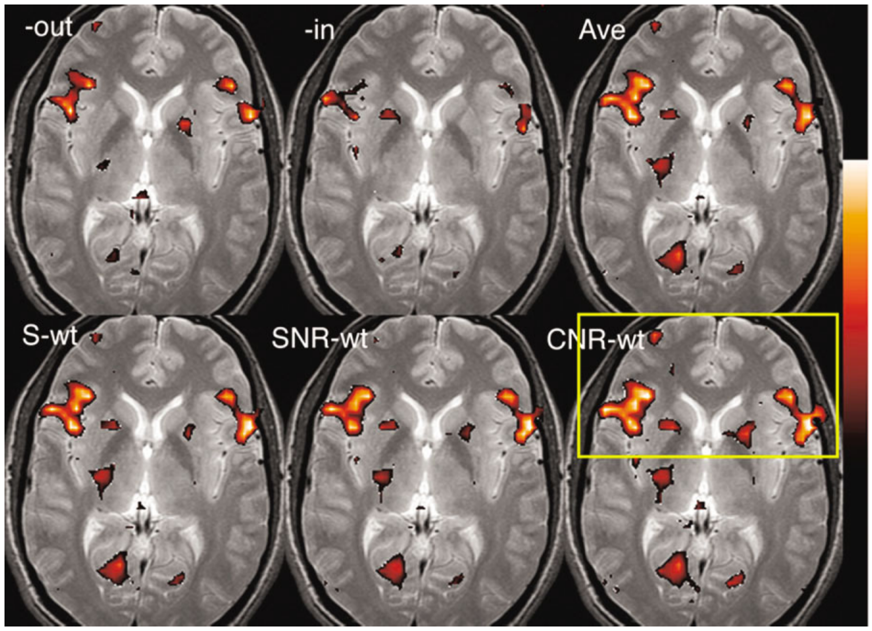

FIG. 1. Activation maps for VWM task, subject 5 showing slice selected for analysis and ROI, for spiral-out and spiral-in components as well as from combination methods. Images are displayed in radiological convention.

Functional acquisitions used FOV 24 cm, BW ± 100 kHz, TE 30 ms. Either 25 (VWM task) or 23 (BH task) contiguous 5 mm slices were acquired with oblique axial scan plane (parallel to AC-PC), using a TR of 2000 ms or 1500 ms, respectively. The spiral-in/out pulse sequence has been described previously (1,2).

Data Analysis

Generation of Time Series

For each subject's scan data, six sets of timeseries were generated by combining the spiral-in and spiral-out timeseries as described above using Ave, S-wt, SNR-wt, and CNR-wt, as well as by simply extracting the spiral-in series and the spiral-out series. Before generating the mean and SD maps, a second-order trend was first removed separately from the spiral-in and spiral-out timeseries using least-squares fits over the full series, and high pass temporal filtering was employed in the noise calculation in order to eliminate variance resulting from the activation signal changes themselves.

Activation Analysis

The timeseries from each scan was analyzed identically. The VWM data were cross-correlated with a covariate *c(t)* developed by convolving a gamma-variate function (7) with the experimental design function. The BH data were cross-correlated with sine and cosine functions at the fundamental task frequency; higher-order harmonics were strongly attenuated because of the hemodynamic filtering and the relatively short block periods and were therefore

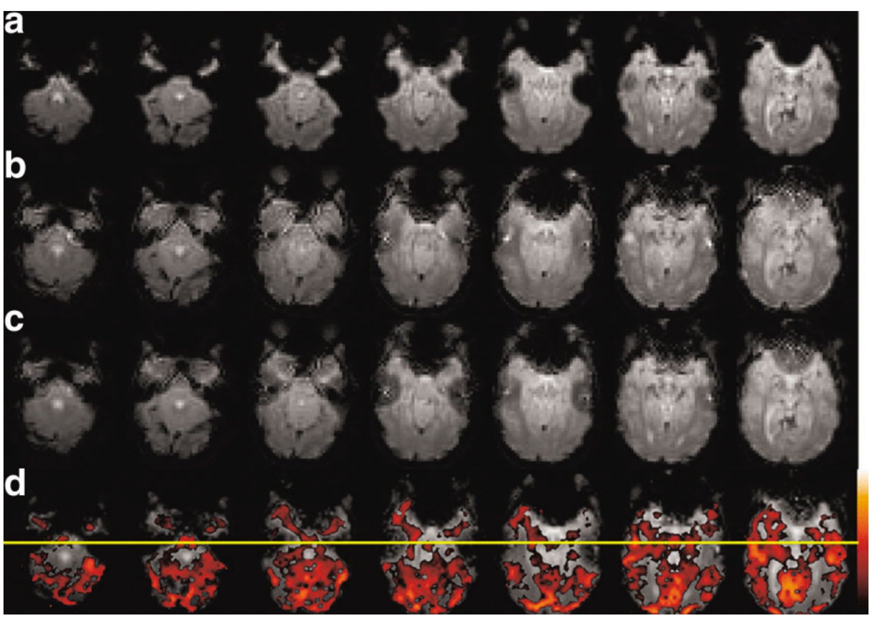

FIG. 2. Seven functional timeseries slices included in analyses of breathholding task for subject 10, showing raw signal intensities for (**a**) spiral-out, (**b**) spiral-in, (**c**) S-wt spiral-in/out. **d:** CNR-wt activation map overlaid on mean images. Only regions above the line were included in the quantitative analysis.

Table 1
Volume of activated voxels normalized to activation volumes for signal-weighted method

Task, ROI		Out	In	Ave	S-wt	SNR-wt	CNR-wt
VWM, whole brain	Mean	0.65	0.52	0.99	1.00	0.92	1.33
	Standard	0.09	0.13	0.03		0.04	0.13
VWM, LPFC	Mean	0.66	0.52	0.92	1.00	0.84	1.59
	Standard	0.21	0.24	0.06		0.17	0.23
BH, PFC	Mean	0.55	0.73	0.94	1.00	0.72	1.46
	Standard	0.14	0.20	0.07		0.13	0.16

not needed. In both cases, a sigma filter was used to cluster pixels in a 3×3 region (8). Activation maps depicting the resulting in-phase correlation coefficients (r) were overlaid on the T_2 images for visual inspection.

Activation volumes were quantified by counting voxels that exceeded a significant correlation coefficient threshold. For the VWM task a "global" analysis was performed for the full brain using $r \geq 0.45$ (significant at $t = 4.4$). A second "regional" analysis was performed using only a single slice in the prefrontal cortex with an ROI chosen to include lateral activation regions and having a significant threshold $r \geq 0.30$ ($t = 2.7$). For BH data, activation volumes were quantified in the frontal region using anterior ROIs in the seven most inferior slices. This choice of ROIs therefore predominantly included cortical regions that were strongly affected by SFG-related signal dropout and were deemed likely to demonstrate the greatest differences between combination methods.

The number of activated voxels so determined was recorded for each of the activation maps and one-tailed, paired (across subjects) *t*-tests were performed to compare the various combination methods. Moreover, for each subject ratios of activation volumes were calculated relative to the signal-weighted combination in order to directly compare alternative combination methods to that which has been shown to demonstrate a clear advantage over spiral-out (1,2).

The relationship between activation amplitude and both image signal amplitude and SNR was examined for the regional VWM data by plotting the activation correlation coefficient for activated voxels for all subjects vs. the signal and SNR for those voxels. Linear regression was performed to determine the degree to which activation was dependent on either signal or SNR.

RESULTS

Figure 1 shows activation maps for a typical subject with the slice chosen for the regional analysis. The CNR-weighted map demonstrates the greatest activation volume, followed by (for this subject) the S-weighted map. Note that all the spiral-in/out activation maps show greater activation than either spiral-out or spiral-in maps, and that spiral-out activation was greater than activation for spiral-in.

Quantification of the VWM data for the whole-brain analysis is shown in Tables 1 and 2. In Table 1 the activation volumes are normalized by dividing by the volumes for the signal-weighted combination. The spiral-out and spiral-in acquisitions demonstrate ~65% and 52% of the activation obtained by the S-weighted spiral-in/out combination, respectively. The Ave and SNR-wt methods provided activation similar to that for the S-wt combination. The CNR method demonstrated greater activation volumes compared with all other methods and 2.0 times that for the spiral-out acquisition. The combination methods are compared by paired *t*-test in Table 2. CNR weighting returns significantly greater activation volumes than the other weighting methods. Furthermore, there is a trend for S-wt to perform better than the simple Ave method, and the SNR method is statistically inferior to the other combination methods (0.92 average activation volume compared with S-wt). Similar results are presented for the single-slice prefrontal region analysis of the same VWM data.

Table 2
Paired *t*-tests comparing activation volume differences between each processing method

Task, ROI	S-wt	SNR-wt	CNR-wt
Ave	S-wt > Ave	Ave > SNR-wt	CNR-wt > Ave
VWM, whole brain	0.094	0.028*	0.0134*
VWM, LPFC	0.041*	0.182	0.004*
BH, PFC	0.032*	0.131	0.002*
S-wt		S-wt > SNR-wt	CNR-wt > S-wt
VWM, whole brain		0.042*	0.010*
VWM, LPFC		0.070	0.004*
BH, PFC		0.016*	0.004*
SNR-wt			CNR-wt > SNR-wt
VWM, whole brain			0.0150*
VWM, LPFC			0.003*
BH, PFC			0.004*

*Significant *P* value.

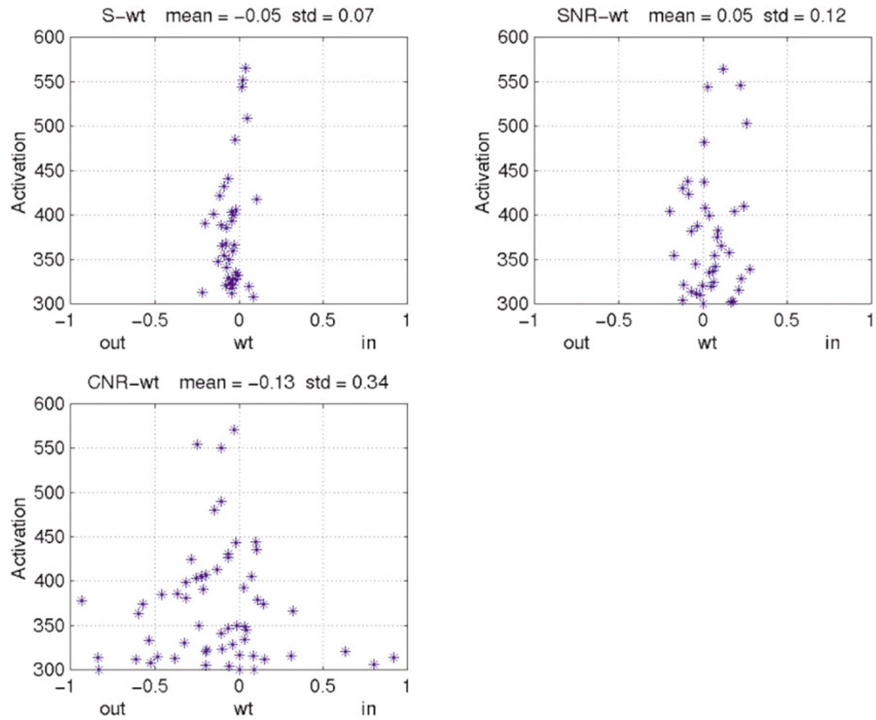

FIG. 3. Plots of regional VWM activation amplitude (cc values ×1000) vs. the weighting in activated voxels for the subject in Fig. 1. Abscissa represents weighting scaled from −1.0 (purely spiral-out) to 1.0 (purely spiral-in), so that 0.0 represents equal weighting. Means and standard deviations of the weighting are also shown.

Again, all spiral-in/out combinations methods provide significantly increased activation over spiral-out or spiral-in, and the CNR-weighted method is strongly superior to other combination methods. The signal-weighted combination was statistically superior to simple averaging and exhibited a strong trend for greater activation than SNR-wt. As with the global analysis of the VWM task, SNR-wt was inferior to the other combinations.

Typical spiral-in, spiral-out, and S-wt "raw" functional images collected in the BH task are shown in Fig. 2, together with an activation map generated by the CNR-wt method overlaid on its mean image. The conclusions reached for the VWM analyses generally hold as well for the breathholding data as summarized in Tables 1 and 2. Note, however, that the BH task provided many more activated voxels than obtained with the VWM task.

Figure 3 shows plots of the activation amplitude (r values) vs. the weighting values for all activated voxels in the regional analysis of VWM data for the subject depicted in Fig. 1. Most voxels received nearly equal weighting of the spiral-in and spiral-out components for the S-weighted method, while the CNR-weighted method shows the broadest distribution of weighting with a small skew towards spiral-out weighting. In all cases the lowest activation values tended to occur in voxels that were dominated by either spiral-in (wt → 1) or spiral-out (wt → −1) contributions.

The correlation between activation amplitude (r) and the image signal intensity for all activated voxels in the regional VWM data pooled over all subjects are shown in Table 3. There is only modest correlation between activation amplitude and signal as shown by the regression correlation values for each of the raw as well as combined timeseries. Similar analysis of activation vs. SNR showed even less correlation (Table 3).

DISCUSSION

In confirmation of earlier results, all spiral-in/out combinations generated significant advantages over spiral-out acquisition; additionally, spiral-in provided less activation than spiral-out in the VWM task. The signal-weighted method (S-wt) performed better than simple averaging (Ave) and, surprisingly, outperformed SNR weighting. The optimal combination of those tested was CNR-weighted, which yielded far greater activation volumes than the other combination methods.

The CNR-weighted method extracts weights from spiral-in and spiral-out timeseries based on the fit of each to a covariate derived from the experimental paradigm. This method therefore directly uses BOLD signal responsiveness in relation to cognitive or physiological test manipulations to determine the amount of each component to use in each voxel. As shown in Fig. 3, the CNR-wt method

Table 3
Correlation coefficients for activation values (r) vs. raw signal and vs. SNR in activated voxels for VWM regional analysis

Correlation	Out	In	Ave	S-wt	SNR-wt	CNR-wt
r vs. signal	0.24	0.44	0.24	0.20	0.23	0.23
r vs. SNR	−0.07	0.21	−0.01	−0.05	−0.09	0.23

tends to use a slightly larger fraction of the spiral-out component. This may be explained by the fact that the BOLD sensitivity of the spiral-in image for uniform brain can be less than that for spiral-out, because the effective echo time is shorter. That is, while the low spatial frequencies are collected at nearly the same time (TE) for the two images, all the rest of the *k*-space data are obtained at times <TE for spiral-in, and >TE for spiral out. Therefore, while the spiral-in image recovers signal in SFG regions that is lost to spiral-out, its BOLD sensitivity is nevertheless reduced because of foreshortened T_2*, as was shown in simulations (1). Also evident in Fig. 3 is the broader dispersion of weights across the two components for CNR-wt, suggesting a more adaptive combination based on the BOLD sensitivity, that may explain its increased effectiveness.

The observation that CNR-weighting returns greater activation than S-wt or SNR-wt methods is consonant with the weak correlation found between BOLD contrast and signal or SNR (Table 3). The explanation for the latter discordance stems in part from blurring and distortion of the images near dropout regions caused by SFGs. In such cases, the signal tends to pile up near the edges of the dropout (e.g., Fig. 2A, slice 7), causing partial volume dilution of the BOLD contrast. At the same time, the signal variance in these voxels is greater than for uniform regions due to heightened sensitivity of the steep intensity gradient to brain pulsatility and to field fluctuations from breathing (9). Since these effects manifest differently in the spiral-in and spiral-out images (Fig. 2a,b), and with the BOLD contrast only weakly coupled to either signal or SNR in such regions, the CNR-weighting provides a superior combination metric.

A potential criticism of CNR-weighting is that the combination is biased by prior information through activation analysis of the two component timeseries. If the individual activation maps contain false-positives due to low statistical power or task-correlated noise, these errors will be propagated into the combined timeseries just as true-positives will, and the stronger of the -in and -out components will be exaggerated. Thus, the increased activation volumes achieved with CNR-wt could include increased false-positives as well. However, there is evidence that the increase in apparent activation is not predominantly such type-II errors. The cluster filtering applied to the activation maps discriminated against single-voxel activations, and inspection of the activation maps revealed that the increased activation volumes generally resulted from increased cluster size rather than more clusters (see Fig. 1).

CONCLUSION

The CNR-wt technique demonstrated strongly significant advantages over other methods including the previously employed S-wt combination, with increases in activation volumes of 33–59% over S-wt for the three task analyses and factors of 100–200% increase over spiral-out alone. We conclude that adaptive combination methods based on statistical weighting may provide improved use of information from spiral-in and spiral-out acquisitions.

REFERENCES

1. Glover GH, Law CS. Spiral-in/out BOLD fMRI for increased SNR and reduced susceptibility artifacts. Magn Reson Med 2001;46:515–522.
2. Preston AR, Thomason ME, Ochsner KN, Cooper JC, Glover GH. Comparison of spiral-in/out and spiral-out BOLD fMRI at 1.5T and 3T. NeuroImage 2004; 21:291–301.
3. Kruger G, Glover G. The physiological noise in oxygen-sensitive magnetic resonance imaging. Magn Reson Med 2001;46:631–637.
4. Kruger G, Kastrup A, Glover G. Neuroimaging at 1.5T and 3.0T: comparison of oxygen-sensitive magnetic resonance imaging. Magn Reson Med 2001;45:594–604.
5. Kastrup A, Krèuger G, Glover GH, Moseley ME. Assessment of cerebral oxidative metabolism with breath holding and fMRI. Magn Reson Med 1999;42:608–611.
6. Kastrup A, Krèuger G, Glover GH, Neumann-Haefelin T, Moseley ME. Regional variability of cerebral blood oxygenation response to hypercapnia. NeuroImage 1999;10:675–681.
7. Friston KJ, Jezzard P, Turner R. Analysis of functional MRI time-series. Hum Brain Map 1994;1:153–171.
8. Glover GH, Lai S. Self-navigated spiral fMRI: interleaved versus single-shot. Magn Reson Med 1998;39:361–368.
9. van de Moortele PF, Pfeuffer J, Hu X, Ugurbil K, Glover G. Respiration induced global B_0 fluctuations in the human brain at 7 Tesla. I. Consequences in fMRI EPI time series. Magn Reson Med 2002;47:888–895.